Int J Clin Exp Pathol 2017;10(5):5092-5104
www.ijcep.com /ISSN:1936-2625/IJCEP0050663

Original Article

Whole-exome sequencing identifies a *de novo* mutation in *TRPM4* involved in pleiotropic ventricular septal defect

Zhen Jia[1,2*], Fengbiao Mao[2,3*], Lu Wang[4], Mingzhen Li[5], Yueyi Shi[6], Baorong Zhang[7], Guolan Gao[1]

Departments of [1]Obstetrics and Gynecology, [7]Stomatology, Beijing Aviation General Hospital, Beijing, China; [2]Beijing Institutes of Life Science, Chinese Academy of Sciences, Beijing, China; [3]University of Chinese Academy of Sciences, Beijing, China; [4]Institute of Life Science, Southeast University, Nanjing, China; [5]Beijing Center for Physical and Chemical Analysis, Beijing, China; [6]Department of Stomatology, The General Hospital of Chinese People's Liberation Army, Beijing, China. [*]Equal contributors.

Received February 12, 2017; Accepted February 25, 2017; Epub May 1, 2017; Published May 15, 2017

Abstract: Background: As a structural defect due to abnormal heart formation, congenital heart disease (CHD) is the most common birth defect. Most of the known causes of congenital heart disease are sporadic genetic changes in results of either focal mutations or deletion. The purpose of this study was to investigate *de novo* mutation of CHD. Methods: Whole exome sequencing analysis was performed on DNA of venous blood of his parents and leg muscles from the child with CHD to scan for *de novo* mutations. Sanger sequencing was performed to verify these candidate mutations in the CHD tissue, parental blood, Clinical and fetal echocardiography examinations were performed on the patient diagnosed with CHD. Results: The sequencing methods found a *de novo* missense mutation c.A25G (p.S9G) in exon 2 of gene *TRPM4*, which plays a critical role in mediating transport of monovalent cations across membranes. The *de novo* missense mutation led to the conversion of serine acid to glycine acid (p.S9G), resulting in a deleterious mutation in the TRPM4 protein. Multiple-sequence alignments showed that codon 9, where the mutation (c.A25G) occurred, was located within a phylogenetically conserved region. Conclusions: We report a *de novo* missense mutation c.A25G (p.S9G) in *TRPM4* for Chinese patient with CHD. Our findings broaden the genotypic spectrum of CHD and provide new molecular insight into future clinical genetic diagnosis of CHD.

Keywords: Congenital heart disease, whole-exome sequencing, *de novo* mutation, TRPM4, pleiotropic ventricular septal defect

Introduction

Congenital heart disease (CHD) is the most common human congenital defect and a leading cause of death in China. With an incidence that varies from 0.8 to 2% in neonates, CHD contributes to a much larger fraction of stillbirths [1, 2]. Until recently, approximately half of the deaths were due to CHD during infancy. Moreover, more than 75% of children suffered from CHD will live into adulthood (3, 4). Recent estimates place the proportion of CHD in adults is approximately 3000 per million [3]. Several factors could account for the rising prevalence of CHD in adults. Firstly, heart defect could be corrected in the majority of cases with the advance in diagnostics and medical and surgical treatments, so that children with CHD could reach adulthood [3]. Secondly, many patients with mild malformations of the heart are not diagnosed until they grow up. Consequently, this population of cardiovascular disease has been increasing by almost 5% per year in the world [4].

To discover the causes of CHD is not only a fundamental research endeavor but also crucial for the healthcare of this growing community [5]. The majority of CHD cases are thought to result from gene mutations on account of observations of Mendelian inheritance of CHD in families. It is supported by that congenital syndromes induced by deletions of chromosomal regions would result in CHD phenotypes as well as several other manifestations. Fortunately, with the developments of next-gen-

eration sequencing and other molecular techniques, it became possible to identify the genetic causes of CHD over the past few decades [6, 7].

Exome sequencing is a transformative technology that enables unbiased detection of mutations on a whole-exome scale. Identification of disease-causing mutations will provide a basis for determining the molecular pathogenesis of CHD and for development of effective therapies [8]. To identify the potential genetic etiology for defects in cardiac embryogenesis and to fully understand the causes and mechanisms of CHD, we applied whole-exome sequencing (WES) and bioinformatics to a recently recruited stillbirth with pleiotropic ventricular septal defect (PVSD). In the present study, we report the identification of heterozygous mutations c.A25G (p.S9G) in *TRPM4* in the stillbirth with ventricular septal defect and report the molecular association of ventricular septal defect with a *de novo* mutation in *TRPM4*.

Materials and methods

Subjects and ethics statement

The subjects included a couple and their child who was diagnosed with congenital atrial septal defects. The stillbirth was diagnosed as pleiotropic ventricular septal defect by ultrasonic examination, and DNA was extracted from the leg muscle of the stillborn fetus. DNA was isolated from venous blood from the father and mother to be used as normal control.

The methods were carried out in accordance with the approved guidelines. This study was approved by the ethical committee of The Beijing Aviation General Hospital. Relevant informed consent was obtained from all participants.

All DNA sequencing data have been deposited in Sequence Read Archive (SRA) with accession numbers of BioSample SAMN03658610 (father), SAMN03658611 (mother), and SAMN03658609 (CHD child) in BioProject PRJNA284111.

Exome sequencing

The DNA from the leg muscle of the stillbirth and venous blood of the parents was used for exome sequencing. Exome sequencing was carried out using an Agilent SureSelect Human All Exon v5.0 (51 M) kit with the protocol from Illumina's TruSeq Exome Enrichment Guide (SureSelectXT Target Enrichment System for Illumina Paired-End Sequencing Library, Agilent). Genomic DNA libraries were prepared according to the manufacturer's instructions (Illumina, USA). The captured library was then sequenced on Illumina HiSeq2000 analyzers with 126 cycles per read, to generate paired-end reads and 8 bp of index tag (following the manufacturer's standard sequencing protocols).

Read mapping and bioinformatics analysis

Image analysis and base calling were performed with Illumina Basecaller program (v1.8). The sequence reads were aligned to the human genome reference obtained from the UCSC database (http://genome.ucsc.edu/), version hg19 (GRCh37), using the BWA aligner program (v0.7.10-r789). Single nucleotide polymorphisms (SNPs) and Short insertions or deletions (InDels) altering coding sequence or splicing sites were identified by GATK (v1.4-33-g051b450) through realignment analysis of insertions and deletions, quality recalibration, and InDels calling (UnifiedGenotyper in GATK). Subsequently, we used VarScan2 v2.3.7 (http://varscan.sourceforge.net/) to detect the *de novo* mutations in the exome data from the trios. We applied varElect (http://varelect.genecards.org/) to select mutations associated with the function of heart development. The effects of candidate mutations on protein features were predicted with the GERP++ program (May 22 2011). Potential rejected substitutions were evaluated by PolyPhen-2 (http://genetics.bwh.harvard.edu/pph2/). The impact of the mutation on RNA secondary structure was determined by RNAsnp v1.2 (http://rth.dk/resources/rnasnp/).

PCR and sanger sequencing

Following the results of exome sequencing, Sanger sequencing was performed to verify the genetic defects. Primers flanking the mutation area of *TRPM4* were designed by Primer Premier 5.0, based on the reference genomic sequences of the human genome from GenBank at the National Center for Biological Information (NCBI), and synthesized by Invitrogen, Shanghai, China. The forward primer was

Table 1. Clinical characteristics of the fetus with pleiotropic ventricular septal defect by diagnosis of ultrasonography

Two-dimensional measurement	Measured value (mm)	Doppler measurement		Measured value (cm/s)
Thoracic horizontal diameter	40.1	Mitral valve	A	36
Cardiac horizontal diameter	24		E	23
Left ventricle	6.9	Tricuspid valve	A	40
Right ventricle	7.2		E	29
Left atrium	8.3	Aorta velocity	-	-
Right atrium	8.8	Pulmonary artery velocity	-	37
Aorta	6.2	Ductus arteriosus	Systolic	41
Aortic isthmus	4.0		Diastolic	5
Descending aorta	4.4	Arcus aortae	Systolic	69
Pulmonary artery	1.7		Diastolic	10
-	-	Fetal heart rate (FHR)		150 bpm
Foramen ovale	6.4	Patent foramen flow tube		-

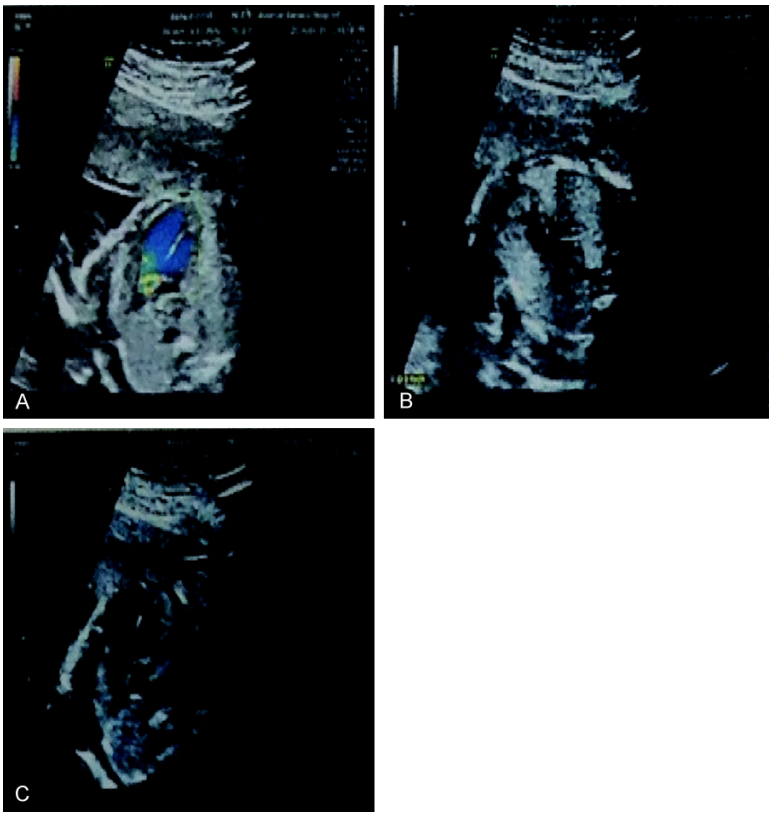

Figure 1. Clinical and fetal echocardiography examinations on the patient diagnosed with CHD. A. Four cavity structure shows clear heart with ventricular septal row at about 0.39 cm. B. Three vessels section showed that the aortic straddles more than 50% with no observation of obvious pulmonary artery. C. Non-standard aspects showed that pulmonary artery trunk and branch structure were likely visible and the trunk diameter was about 0.15 cm but without blood flow signal. Pericardial cavity was shown a dark liquid area of about 0.3 cm wide.

5'-CATGGTGGTGCCGGAGAAGG-3', and the reverse primer was 5'-GGAAAGAAGCAGAACCGAGCC-3'. PCR amplification was carried out using an Applied Biosystems Inc. (ABI) 9700 Thermal Cycler. PCR products were directly sequenced on an ABI PRISM 37-30 automated sequencer (Applied Biosystems).

Results

Clinical presentations

The subject was a four-month fetus recruited from a Chinese family; the mother was 28 years old. At four months of pregnancy, the fetus was diagnosed at low risk for Down syndrome. The ultrasound examination of fetal cardiac structure performed at Beijing Aviation General Hospital showed heart abnormalities including ventricular septal, aortic saddle, and pulmonary artery occlusion. The results of B ultrasound by Beijing Anzhen Hospital were double-checked and indicated that the fetus had PVSD along with aortic saddle, pulmonary artery occlusion, and a large-diameter of the oval foramen (**Table 1**).

The detailed diagnostic information includes: 1) Most of the fetal heart was located in the left

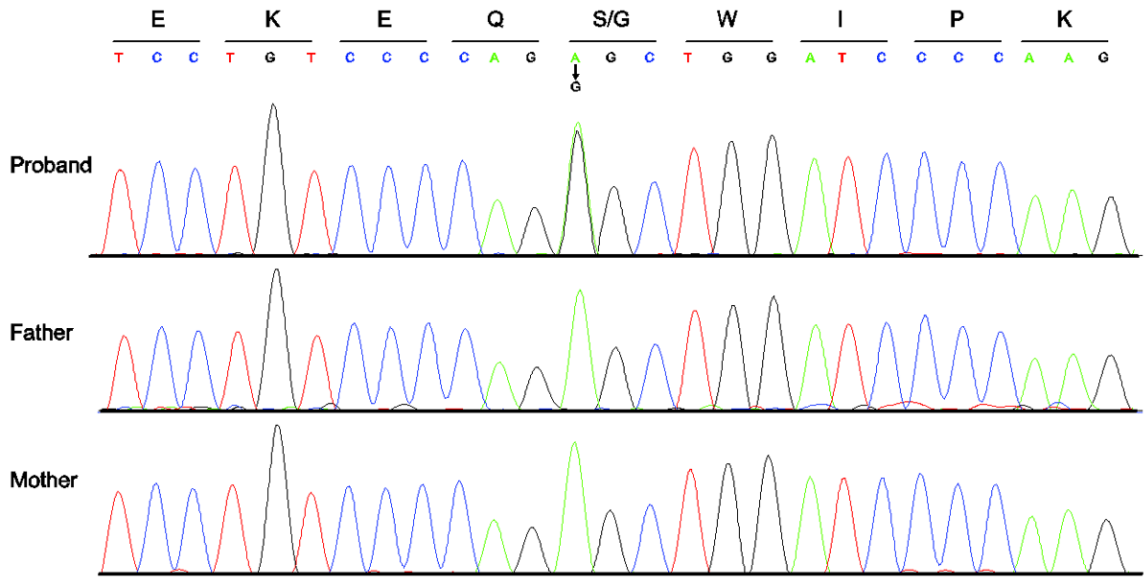

Figure 2. DNA sequence chromatograms of the normal parents and the affected child are shown. The c.A25G mutation, which is located in exon 2 of TRPM4, has been identified as a de novo missense mutation.

chest, apical facing left. The cardiothoracic ratio was in good condition. In the ultrasound, the left ventricle was hyperechoic with a size of 1.9 mm (**Figure 1A**). 2) The left atrium was located in front of the spine with foramen ovale of valve flap. The right ventricle was located behind the sternum. The left and right atrioventricular ratio was normal. The aorta was broadening forward straddle on ventricular septum without an exact pulmonary opening. The pulmonary artery narrowed by about 1.7 mm. Color Doppler flow imaging (CDFI) presented retrograde perfusion signals of blood flow from the pulmonary artery (**Figure 1B**). 3) The atrial septal and orthogonal structure existed. The position, shape, and opening of the atrioventricular valve appeared normal. The CDFI did not show abnormal regurgitating signal for the atrioventricular valve. 4) There were sustaining breaks of about 5.5 mm in the upper region of the interventricular septum. The CDFI of atrioventricular showed a bidirectional shunt signal in the horizon (**Figure 1C**). 5) The fetal heart rate (FHR) was 150 bpm without heart arrhythmia.

Mutation identification

To identify potential causative mutations, we performed whole-exome sequencing of DNA from three members of the family, using DNA from the leg muscle of the stillborn and the venous blood of the parents. We generated 7.63, 7.75, and 9.11 billion bases of 125-bp paired-end read sequences for the stillbirth, the father, and mother, respectively. Among the raw data, 7.62 (99.8%), 7.73 (99.7%), and 9.10 (99.8%) billion bases (stillbirth, father, and mother, respectively) passed the quality assessment. 7.44 (97.51%), 7.56 (97.57%), and 8.88 (97.48%) billion bases aligned to the human reference for the stillbirth, the father, and mother, respectively.

The sequencing results from the stillbirth showed that 4.09 billion bases (54.91%) mapped to the targeted region (46.21 Mb) with a mean coverage of 44.25-fold. A total of 21,010 single nucleotide variants (SNVs; missense, nonsense, and splice site mutations) and 1,227 InDels (short coding insertions or deletions) were identified. Among the SNVs, 6,597 nonsynonymous variants were identified in either the coding regions or the splice sites in the stillbirth. In the father's sample, 3.89 billion bases (51.55%) mapped to the targeted region with a mean coverage of 42.09-fold. A total of 22,902 SNVs and 1,218 InDels were identified. Among the SNVs, 7,019 nonsynonymous variants were identified in either the coding regions or the splice sites from the father. The mother's sequencing results showed that 4.91 billion bases (55.30%) mapped to the targeted region with a mean coverage of 53.13-fold. A total of 23,489 SNVs and 1,393

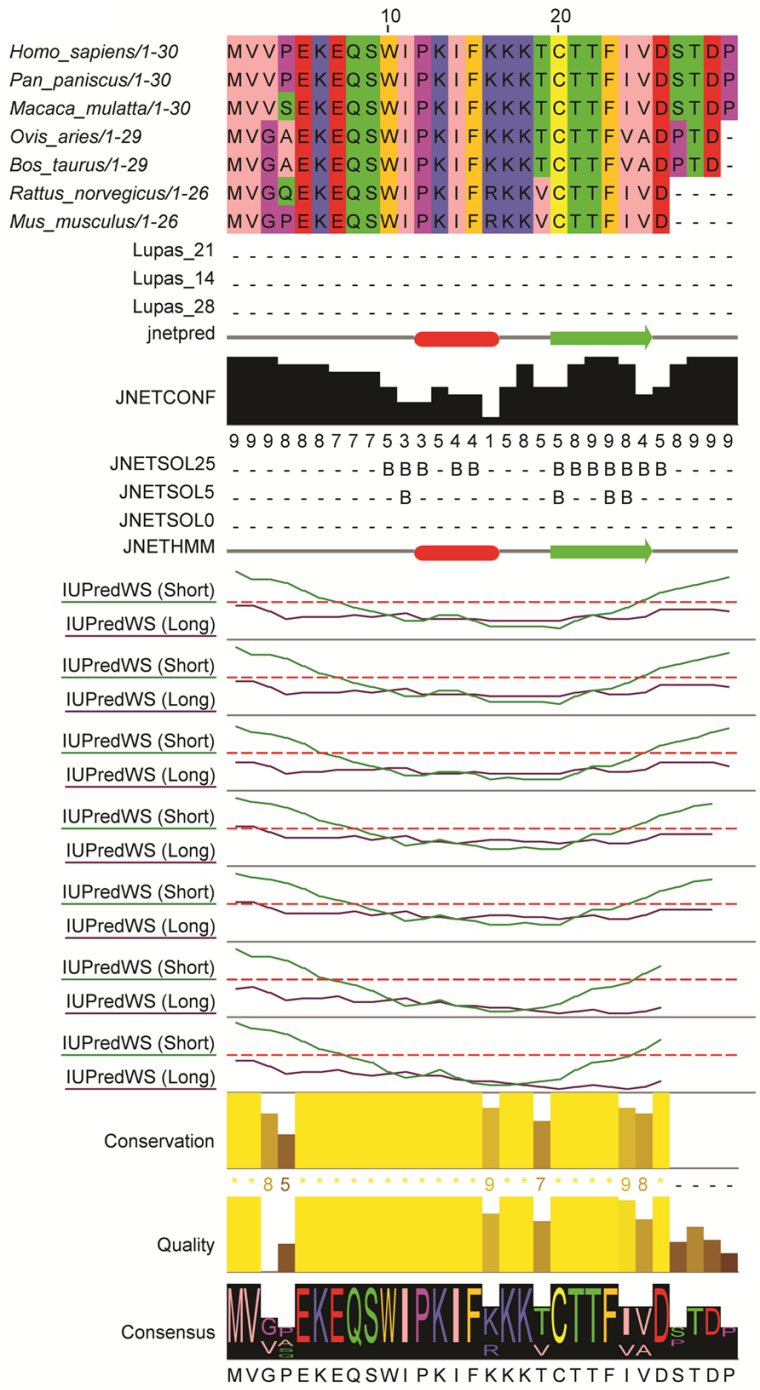

Figure 3. Multiple sequence alignment of seven different biological sequences, corresponding to Homo sapiens, Pan paniscus, Macaca mulatta, Ovis aries, Bos Taurus, Rattus norvegicus, and Mus musculus, respectively, present in order from top to bottom.

InDels were identified; among the SNVs, 7,176 nonsynonymous variants were identified in either the coding regions or the splice sites.

A prioritization framework was applied to identify the pathogenic mutation in the stillbirth, similar to recent studies [9, 10]. We excluded known variants deposited in dbSNP138, 1000 Genomes data, HapMap, and ESP-6500 datasets. After filtering variants displayed in the parents, we obtained 511 candidates for *de novo* mutations in the stillbirth (data not shown). Subsequently, we applied varElect software to select mutations associated with the function of heart development and acquired 7 candidate causal genes with *de novo* mutations (data not shown). Finally, a missense mutation, c.A25G, was confirmed in exon 2 of the TRPM4 gene (GenBank acc. no., NM_001195227) in the stillbirth by validation using bidirectional Sanger sequencing (**Figure 2**). This mutation changed codon 9 AGC, coding for serine, to GGC, which codes for glycine (p.S9G), resulting in a missense mutation. This mutation is predicted to be deleterious or disease-causing by two different programs, i.e., Polyphen-2 (probably damaging with a score of 0.991) and MutationTaster (disease-causing with a score of 1.0). In addition, this mutation was not found in dbSNP138, 1000 Genome, ESP6500, or the in-house exome database, suggesting that it is a rare SNV, which may have contributed to the phenotype of PVSD in the stillbirth.

Bioinformatics analysis of TRPM4 mutations in CHD

We obtained TRPM4 family protein sequences by using BLAST from the NCBI website and employed the software Jal view to perform multiple-sequence alignments in various animal species, including *Homo sapiens*, *Pan paniscus*, *Macaca mulatta*, *Ovis aries*, *Bos Taurus*, *Rattus norvegicus*, and *Mus musculus* (**Figure 3**). The p.Ser9

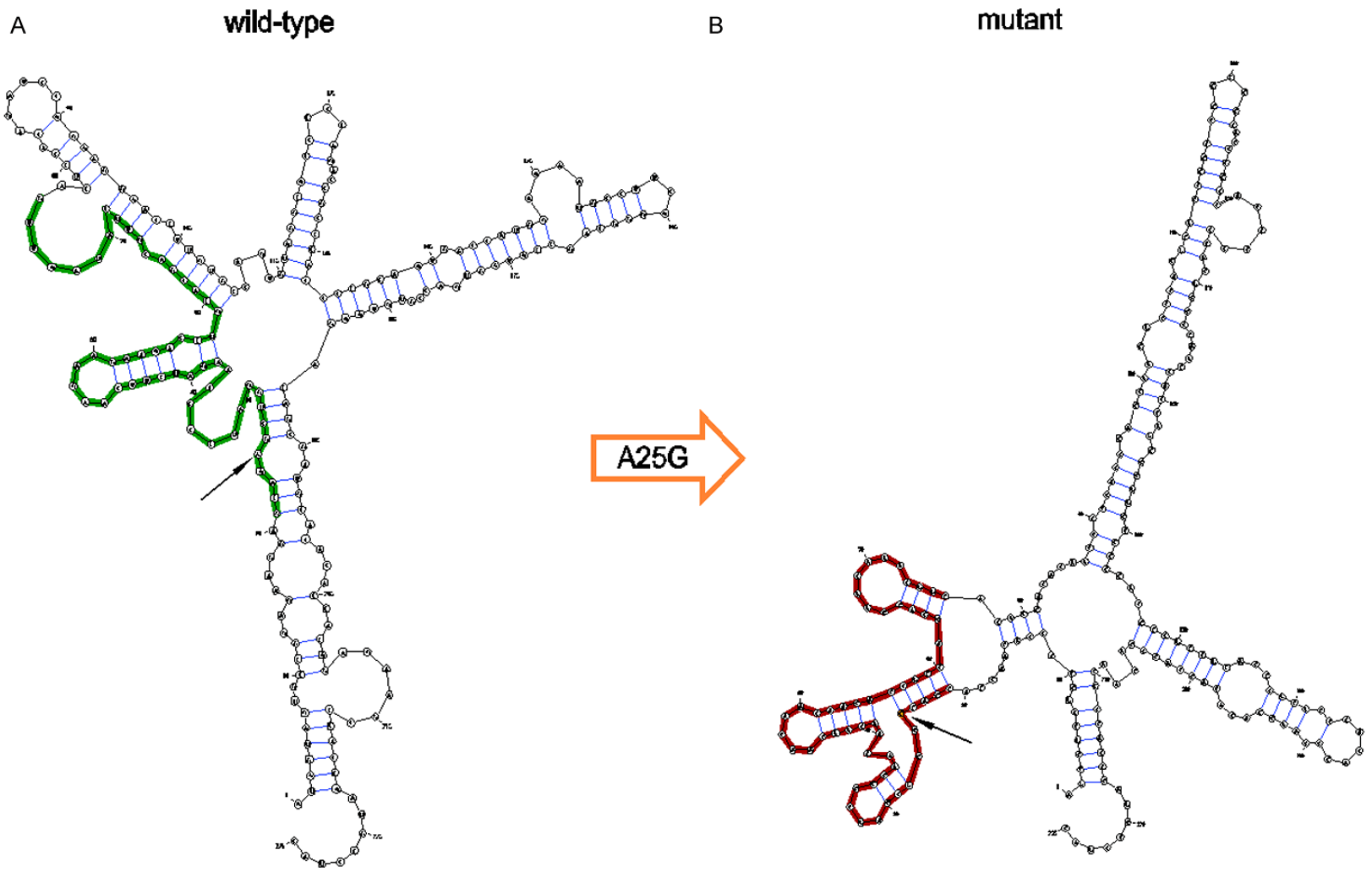
A
wild-type
B
mutant
A25G

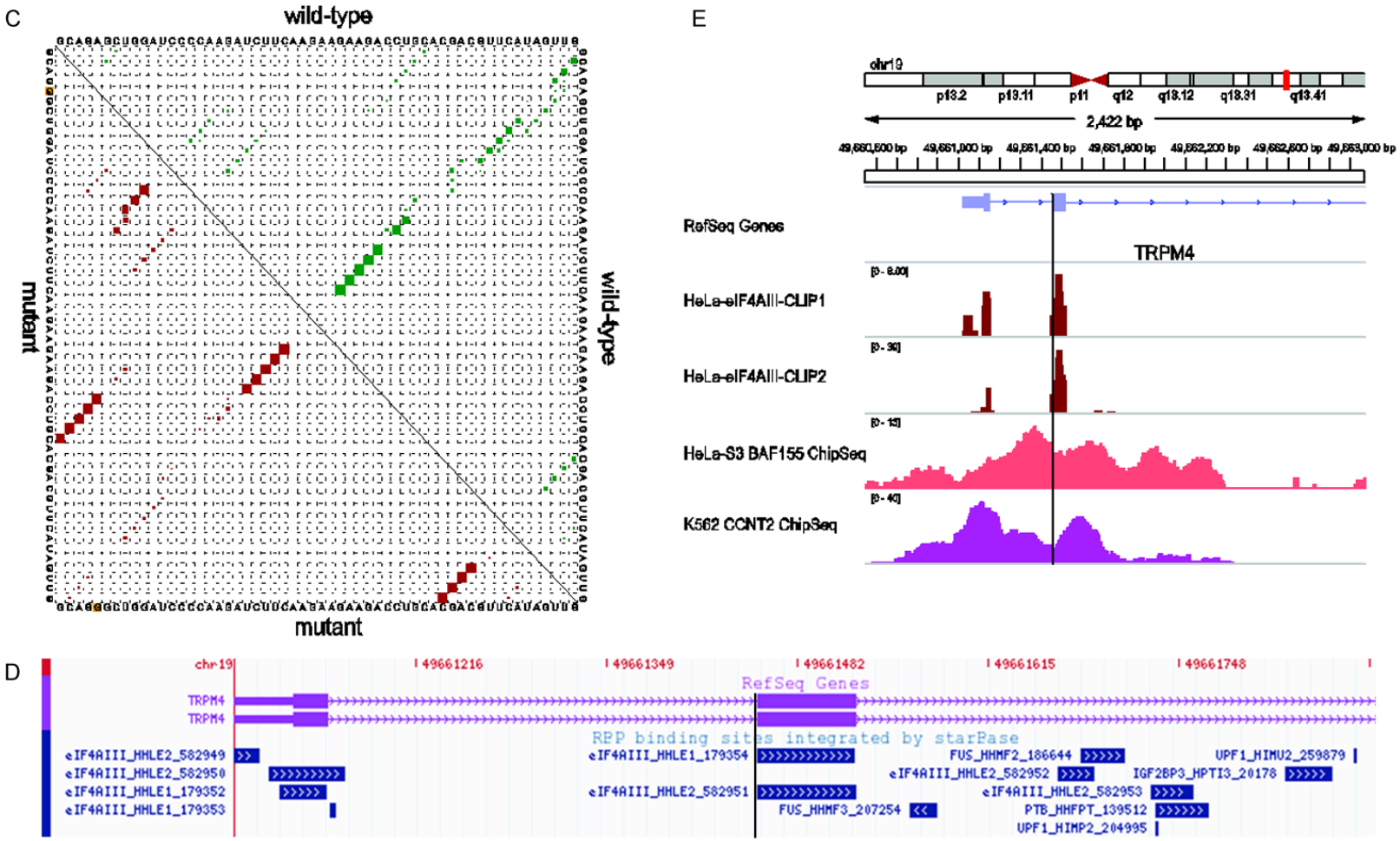

Figure 4. A, B. The structural damage resulting from the c.A25G mutant variant located at the secondary RNA structure of TRPM4. Structures were modeled on the secondary structure of the normal and mutated structure of TRPM4. C. Dot plot shows the corresponding RNA secondary structure base pair probabilities of wild type (upper triangle) and mutant (lower triangle) RNA sequences, respectively. D. RBP-binding site at c.A25G mutant location integrated by starBase (29). The binding sites of eIF4AIII were located in the mutation site in Hela cell. E. RBP-binding signal derived from Par-CLIP at c.A25G mutant location integrated by RBP-Var (30).

Gly variant was found to be located in a highly conserved region of the TRPM4 protein, suggesting its importance for structure and function of TRPM4. This mutation was predicted to affect the protein features and be rejected substitutions predicted by GERP++ with a score of 4.56 (data not shown).

Just as SNPs can affect protein structure and function, the potential impact of SNPs on RNA structure and gene regulation has been considered for decades and widely studied in recent years [11-14]. RNA structure is crucial for gene regulation and function [15]. Therefore, we investigated the influence of c.A25G on the secondary RNA structure of *TRPM4*. Intriguingly, we found that this mutation may play an important role in the complicated and functional RNA secondary structures, possibly giving rise to alteration in the function of RNAs (**Figure 4A** and **4B**). Analysis of base-pair probabilities of the local region revealed that probabilities of mutant sequences were significantly altered compared with that of wild-type sequences (**Figure 4C**).

Therefore, we hypothesized that the alteration of the secondary structure could affect the binding intensity or accessibility of RNA binding proteins (RBPs). Subsequently, we investigate which RBPs could bind the region of this mutation in cell lines from database starBase and found that RBP eIF4AIII were enriched in the locus of mutation in Hela cell lines (**Figure 4D** and **4E**). The RBP eIF4AIII are implicated in a number of cellular processes involving alteration of RNA secondary structure, such as translation initiation, nuclear and mitochondrial splicing, and ribosome and spliceosome assembly. RBP eIF4AIII is a member of the DEAD box protein family. Based on their distribution patterns, some members of this family are believed to be involved in embryogenesis, spermatogenesis, and cellular growth and division [16]. Consequently, we speculated that the mutation of *TRPM4* may impact the binding of RBPs such as RBP eIF4AIII by transforming the RNA secondary structure and result in dysregulation of translation and embryogenesis.

Meanwhile, we also observed two DNA binding proteins BAF155 and CCNT2 could enrich in the region the mutation of *TRPM4* in Hela and K562 cell lines, respectively (**Figure 4E**). Gene ontology (GO) annotations related to *TRPM4* include calcium-activated cation channel activity and calmodulin binding. However, it is unclear which histone modifications regulate the expression of *TRPM4* and which transcriptional factors are associated with the mutation locus of *TRPM4*. By examining the integrated analysis of the data for histone modifications deposited in the Encyclopedia of DNA Elements project (ENCODE) [17], we found that histone modifications at the *TRPM4* locus and the c.A25G mutant variant include H3K27ac, H3K9ac, and H3K4me2/3 in the cell line K562 (**Figure 5**). As those histone modifications are canonically active molecular markers (**Figure 6A**) [18], we speculated that the c.A25G variant might influence the histone modification and affect the expression of *TRPM4*. This is proposed with the caveat that the histone modification data are from cell lines rather than heart tissues. Indeed, the expression of *TRPM4* by PCR validation decreased in CHD fetal compared with that of normal heart tissues deposited in RNA atlas [19]. Similarly, several transcription factors deposited in the ENCODE project [17] are enriched in a locus where the c.A25G variant occurred in *TRPM4* for the cell line K562 (**Figure 6**). These transcription factors are MAZ, PHF8, CHD1, RBBP5, c-Myc, ZBTB7A, NRSF, and REST (**Figure 6B**). These transcription factors binding to the specific regions adjacent to codon 9 of *TRPM4* may presumably function to regulate the transcription of the gene. Due to the vital roles those transcription factors and histones play during the process of cellular function and development, we postulate that the c.A25G variant located in *TRPM4* may have a critical biological impact to explore.

Discussion

Ventricular septal defect (VSD) is the most common form of congenital cardiovascular malformation and an important contributor to the substantially increased morbidity and mortality in infants [20]. In the present study, we report a previously unrecognized missense mutation of p.S9G in TRPM4 identified in a family with congenital PVSD. A cross-species alignment of TRPM4 protein sequences adjacent the mutation showed that the altered amino acid was evolutionarily highly conserved. The p.S9G variant was predicted to be pathogenic by MutationTaster, and the functional analysis substantiated that the p.S9G TRPM4 was

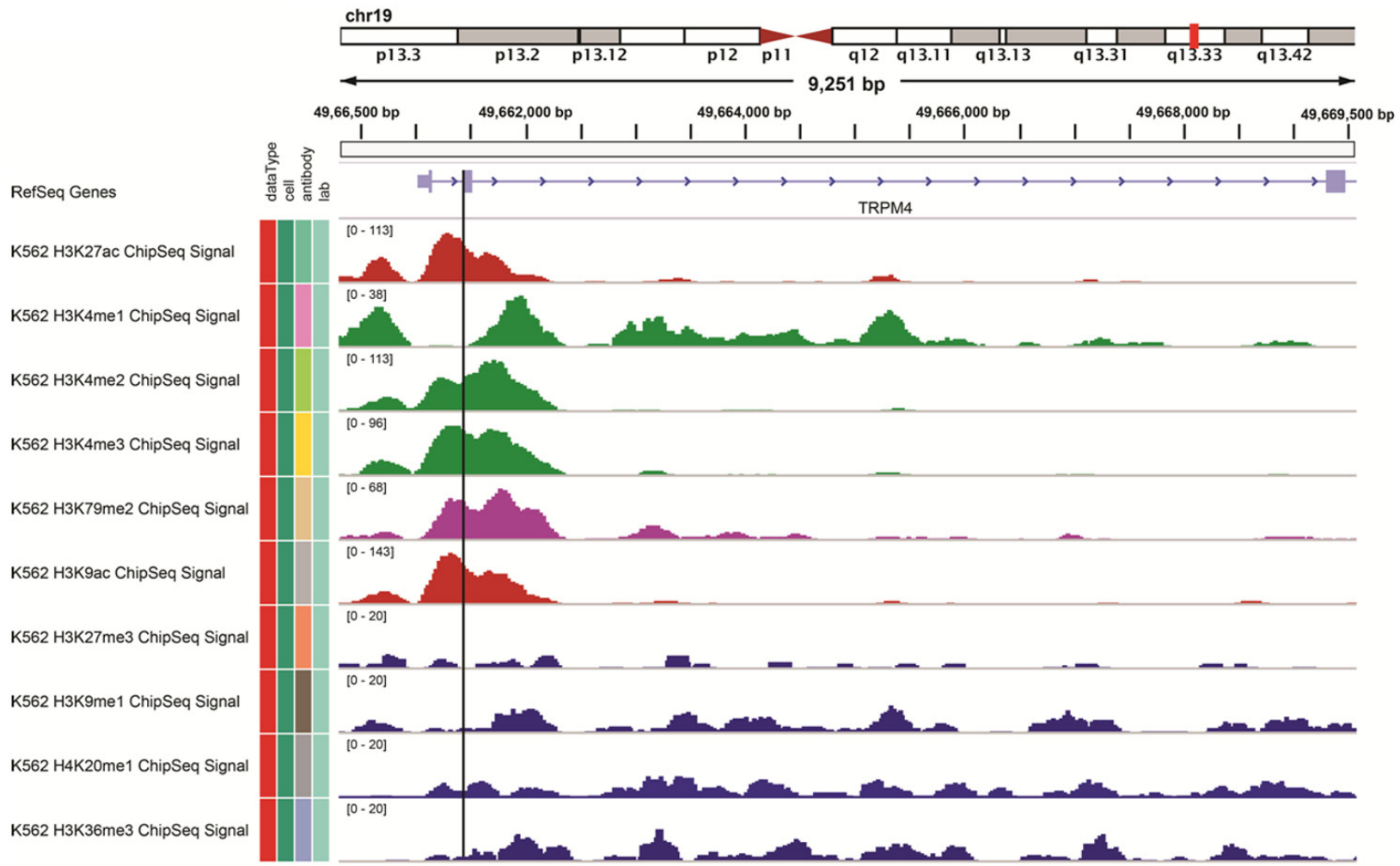

Figure 5. Through the technology of ChIP-seq, histones, such as H3K27ac, H3K9ac, and H3K4me2/3, in cell line K562 were detected to be bound at the site of the c.A25G mutant variant.

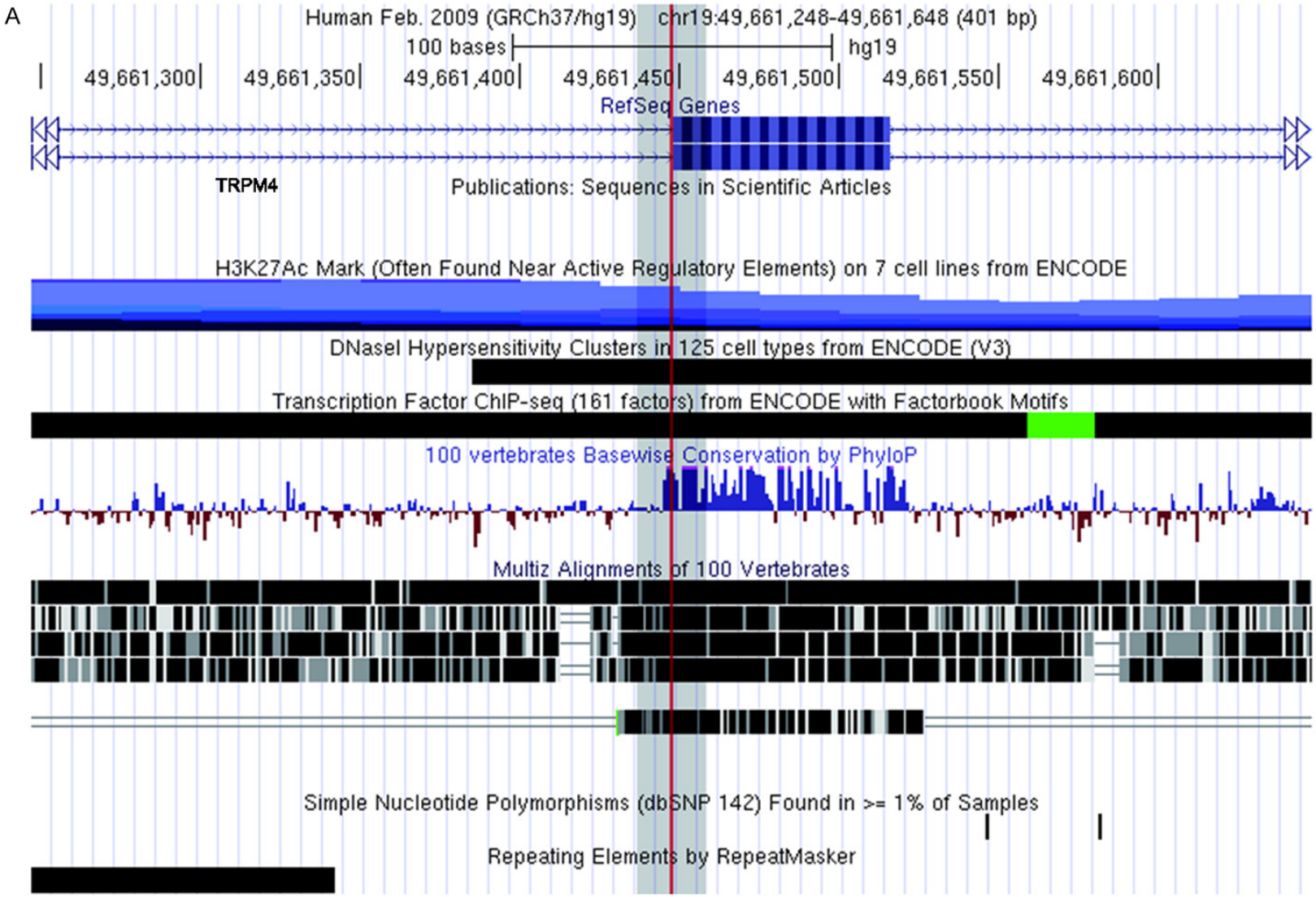
A
Human Feb. 2009 (GRCh37/hg19) chr19:49,661,248-49,661,648 (401 bp)
100 bases
hg19
49,661,300
49,661,350
49,661,400
49,661,450
49,661,500
49,661,550
49,661,600
RefSeq Genes
TRPM4
Publications: Sequences in Scientific Articles
H3K27Ac Mark (Often Found Near Active Regulatory Elements) on 7 cell lines from ENCODE
DNaseI Hypersensitivity Clusters in 125 cell types from ENCODE (V3)
Transcription Factor ChIP-seq (161 factors) from ENCODE with Factorbook Motifs
100 vertebrates Basewise Conservation by PhyloP
Multiz Alignments of 100 Vertebrates
Simple Nucleotide Polymorphisms (dbSNP 142) Found in >= 1% of Samples
Repeating Elements by RepeatMasker

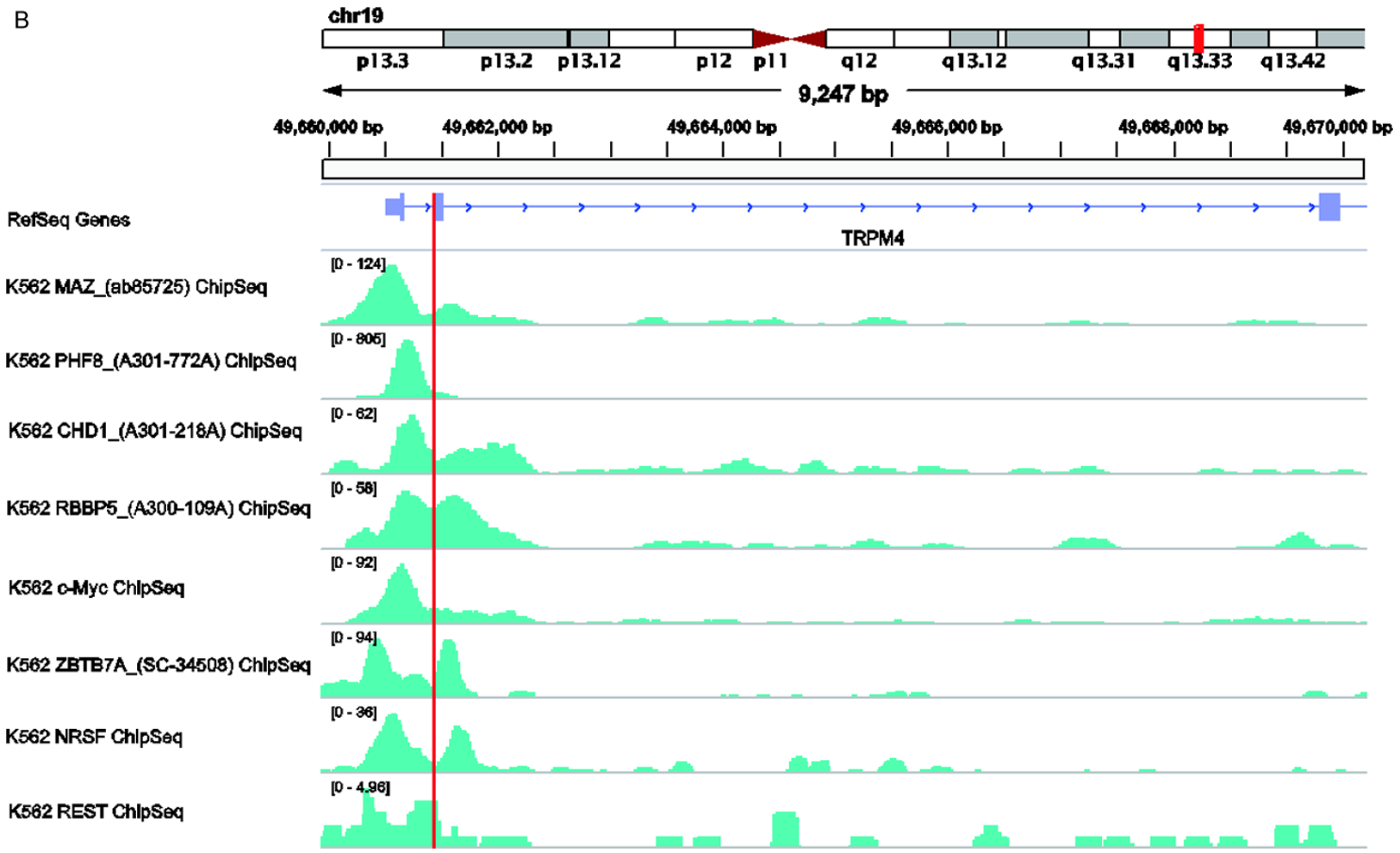

Figure 6. UCSC genome browser data showing selected gene annotation and ENCODE-related tracks for the c.A25G mutation located in TRPM4 gene. A. Histone modification or Transcription factors binding signal derived from ENCODE (31) at c.A25G mutant location integrated by RegulomeDB (32). This mutation locates on the H3K27Ac modification regions and multiple TFs. B. Transcription factors signal derived from ENCODE Chip-seq of K256 cell at c.A25G mutant location integrated by RegulomeDB. The enriched transcription factors include MAZ, PHF8, CHD1, RBBP5, c-Myc, ZBTB7A, NRSF and REST.

associated with significantly decreased transcriptional activity. Therefore, it is very likely that dysfunctional TRPM4 is responsible for PVSD in this family.

Impaired endocytosis of the ion channel TRPM4 is associated with human progressive familial heart block type I [21]. Gain-of-function mutations in TRPM4 cause autosomal dominant isolated cardiac conduction disease [22]. TRPM4 gene mutations appear to play a major role in cardiac conduction disease but not for other related syndromes so far [23]. The phenotypes are variable and clearly suggestive of additional factors modulating the disease phenotype in some patients.

By integrated analysis of whole-exome sequencing data with dataset from starBase and ENCODE, we revealed a novel *de novo* mutation occurred in TRPM4 might play significant role in defect of heart development by aberrant modulating of RNA secondary structure and binding of RBPs as well as chromatin modification. The molecule mechanism of induction of CHD by p.S9G variant in TRPM4 need to be further investigated in the condition that the PAR-CLIP data and histone modification data we employed were derived from cell lines rather than corresponding heart tissues. Current research has explored all of these possible mechanisms with a wide array of technologies that are better than ever, and hence, the future decade promises a nearly complete understanding of heart development and the genetic basis of CHD. Our findings broaden the genotypic spectrum of CHD and provide new molecular insight into future clinical genetic diagnosis of CHD.

Acknowledgements

We thank all probands for their participation. This work was supported in part by grants from the China National Basic Research Program (2013CB535001) and the National Natural Science Foundation of China (81060095).

Disclosure of conflict of interest

None.

Address correspondence to: Dr. Guolan Gao, Department of Obstetrics and Gynecology, Beijing Aviation General Hospital, 3 Anwai Beiyuan Road, Chaoyang District, Beijing 100012, China. Tel: +86-10-59520-088; E-mail: gaoguolanhk@163.com; Dr. Baorong Zhang, Department of Stomatology, Beijing Aviation General Hospital, 3 Anwai Beiyuan Road, Chaoyang District, Beijing 100012, China. E-mail: zhangbrhk@163.com

References

[1] Goldmuntz E. The epidemiology and genetics of congenital heart disease. Clin Perinatol 2001; 28: 1-10.
[2] Loffredo CA. Epidemiology of cardiovascular malformations: prevalence and risk factors. Am J Med Genet 2000; 97: 319-325.
[3] van der Bom T, Zomer AC, Zwinderman AH, Meijboom FJ, Bouma BJ, Mulder BJ. The changing epidemiology of congenital heart disease. Nat Rev Cardiol 2011; 8: 50-60.
[4] Brickner ME, Hillis LD, Lange RA. Congenital heart disease in adults: first of two parts. N Engl J Med 2000; 342: 256-263.
[5] Fahed AC, Gelb BD, Seidman JG, Seidman CE. Genetics of congenital heart disease: the glass half empty. Circ Res 2013; 112: E182-E182.
[6] Blue GM, Kirk EP, Giannoulatou E, Dunwoodie SL, Ho JW, Hilton DC, White SM, Sholler GF, Harvey RP, Winlaw DS. Targeted next-generation sequencing identifies pathogenic variants in familial congenital heart disease. J Am Coll Cardiol 2014; 64: 2498-2506.
[7] Bowles NE. Next generation sequencing analysis of families with congenital heart disease. Cardiology 2014; 128: 243-243.
[8] Evans JP. Finding common ground. Genet Med 2013; 15: 852-853.
[9] Gilissen C, Arts HH, Hoischen A, Spruijt L, Mans DA, Arts P, van Lier B, Steehouwer M, van Reeuwijk J, Kant SG, Roepman R, Knoers NV, Veltman JA, Brunner HG. Exome sequencing identifies WDR35 variants involved in sensenbrenner syndrome. Am J Hum Genet 2010; 87: 418-423.
[10] Guo Y, Yuan J, Liang H, Xiao J, Xu H, Yuan L, Gao K, Wu B, Tang Y, Li X, Deng H. Identification of a novel COL4A5 mutation in a Chinese family with X-linked Alport syndrome using exome sequencing. Mol Biol Rep 2014; 41: 3631-3635.
[11] Halvorsen M, Martin JS, Broadaway S, Laederach A. Disease-associated mutations that alter the RNA structural ensemble. PLoS Genet 2010; 6: e1001074.
[12] Sabarinathan R, Tafer H, Seemann SE, Hofacker IL, Stadler PF, Gorodkin J. RNAsnp: efficient detection of local RNA secondary structure changes induced by SNPs. Hum Mutat 2013; 34: 546-556.
[13] Sabarinathan R, Wenzel A, Novotny P, Tang X, Kalari KR, Gorodkin J. Transcriptome-wide

analysis of UTRs in non-small cell lung cancer reveals cancer-related genes with SNV-induced changes on RNA secondary structure and miRNA target sites. PLoS One 2014; 9: e82699.

[14] Corley M, Solem A, Qu K, Chang HY, Laederach A. Detecting riboSNitches with RNA folding algorithms: a genome-wide benchmark. Nucleic Acids Res 2015; 43: 1859-1868.

[15] Wan Y, Kertesz M, Spitale RC, Segal E, Chang HY. Understanding the transcriptome through RNA structure. Nat Rev Genet 2011; 12: 641-655.

[16] Sauliere J, Murigneux V, Wang Z, Marquenet E, Barbosa I, Le Tonquèze O, Audic Y, Paillard L, Roest Crollius H, Le Hir H. CLIP-seq of eIF4AIII reveals transcriptome-wide mapping of the human exon junction complex. Nat Struct Mol Biol 2012; 19: 1124-31.

[17] ENCODE Project Consortium. The ENCODE (ENCyclopedia of DNA elements) Project. Science 2004; 306: 636-640.

[18] Zhou VW, Goren A, Bernstein BE. Charting histone modifications and the functional organization of mammalian genomes. Nat Rev Genet 2011; 12: 7-18.

[19] Krupp M, Marquardt JU, Sahin U, Galle PR, Castle J, Teufel A. RNA-Seq Atlas-a reference database for gene expression profiling in normal tissue by next-generation sequencing. Bioinformatics 2012; 28: 1184-1185.

[20] Zheng GF, Wei D, Zhao H, Zhou N, Yang YQ, Liu XY. A novel GATA6 mutation associated with congenital ventricular septal defect. Int J Mol Med 2012; 29: 1065-1071.

[21] Kruse M, Schulze-Bahr E, Corfield V, Beckmann A, Stallmeyer B, Kurtbay G, Ohmert I, Schulze-Bahr E, Brink P, Pongs O. Impaired endocytosis of the ion channel TRPM4 is associated with human progressive familial heart block type I. J Clin Invest 2009; 119: 2737-2744.

[22] Liu H, El Zein L, Kruse M, Guinamard R, Beckmann A, Bozio A, Kurtbay G, Mégarbané A, Ohmert I, Blaysat G, Villain E, Pongs O, Bouvagnet P. Gain-of-function mutations in TRPM4 cause autosomal dominant isolated cardiac conduction disease. Circ Cardiovasc Genet 2010; 3: 374-U326.

[23] Stallmeyer B, Zumhagen S, Denjoy I, Duthoit G, Hébert JL, Ferrer X, Maugenre S, Schmitz W, Kirchhefer U, Schulze-Bahr E, Guicheney P, Schulze-Bahr E. Mutational spectrum in the Ca2+-activated cation channel gene TRPM4 in patients with cardiac conductance disturbances. Hum Mutat 2012; 33: 109-117.